Glucagon-Like Peptide 1 Stimulates Insulin Secretion via Inhibiting RhoA/ROCK Signaling and Disassembling Glucotoxicity-Induced Stress Fibers

Kong, Xiangchen; Yan, Dan; Sun, Jiangming; Wu, Xuerui; Mulder, Hindrik; Hua, Xianxin; Ma, Xiaosong

Published in:
Endocrinology

DOI:
10.1210/en.2014-1314

2014

Glucagon-Like Peptide 1 Stimulates Insulin Secretion via Inhibiting RhoA/ROCK Signaling and Disassembling Glucotoxicity-Induced Stress Fibers

Xiangchen Kong,* Dan Yan,* Jiangming Sun, Xuerui Wu, Hindrik Mulder, Xianxin Hua, and Xiaosong Ma

Shenzhen University Diabetes Center (X.K., D.Y., X.W., X.H., X.M.) and Shenzhen University, Shenzhen 518060, People's Republic of China; Lund University Diabetes Centre (J.S., H.M.), Unit of Molecular Metabolism, SE-205 02 Malmö, Sweden; and University of Pennsylvania Perelman School of Medicine (X.H.), Philadelphia, Pennsylvania 19104

Chronic hyperglycemia leads to pancreatic β-cell dysfunction characterized by diminished glucose-stimulated insulin secretion (GSIS), but the precise cellular processes involved are largely unknown. Here we show that pancreatic β-cells chronically exposed to a high glucose level displayed substantially increased amounts of stress fibers compared with β-cells cultured at a low glucose level. β-Cells at high glucose were refractory to glucose-induced actin cytoskeleton remodeling and insulin secretion. Importantly, F-actin depolymerization by either cytochalasin B or latrunculin B restored glucotoxicity-diminished GSIS. The effects of glucotoxicity on increasing stress fibers and reducing GSIS were reversed by Y-27632, a Rho-associated kinase (ROCK)-specific inhibitor, which caused actin depolymerization and enhanced GSIS. Notably, glucagon-like peptide-1-(7–36) amide (GLP-1), a peptide hormone that stimulates GSIS at both normal and hyperglycemic conditions, also reversed glucotoxicity-induced increase of stress fibers and reduction of GSIS. In addition, GLP-1 inhibited glucotoxicity-induced activation of RhoA/ROCK and thereby resulted in actin depolymerization and potentiation of GSIS. Furthermore, this effect of GLP-1 was mimicked by cAMP-increasing agents forskolin and 3-isobutyl-1-methylxanthine as well as the protein kinase A agonist 6-Bnz-cAMP-AM whereas it was abolished by the protein kinase A inhibitor Rp-Adenosine 3′,5′-cyclic monophosphorothioate triethylammonium salt. To establish a clinical relevance of our findings, we examined the association of genetic variants of RhoA/ROCK with metabolic traits in homeostasis model assessment index of insulin resistance. Several single-nucleotide polymorphisms in and around *RHOA* were associated with elevated fasting insulin and homeostasis model assessment index of insulin resistance, suggesting a possible role in metabolic dysregulation. Collectively these findings unravel a novel mechanism whereby GLP-1 potentiates glucotoxicity-diminished GSIS by depolymerizing F-actin cytoskeleton via protein kinase A-mediated inhibition of the RhoA-ROCK signaling pathway. **(*Endocrinology* 155: 4676–4685, 2014)**

Chronic exposure to high glucose, termed glucotoxicity (1), reduces glucose-stimulated insulin secretion (GSIS) in INS-1 cells (2) and islets (3). The impaired secretory capacity of β-cells in glucotoxicity has been suggested to involve in disruptions of the exocytotic machinery (4).

In response to glucose stimulation, insulin-containing granules undergo tightly regulated exocytosis (5). It is known that filamentous actin (F-actin) functions as a negative regulator of exocytosis in pancreatic β-cells (6). Indeed, F-actin is organized as a dense web beneath the plasma membrane and limits the access of insulin-containing granules to the plasma membrane (7, 8). Thus, disruption of the F-actin by latrunculin B (9), or cytochalasins (10) enhances GSIS. In contrast, stabilization of the F-actin with jasplakinolide inhibited KCl-stimulated insulin secretion (11, 12). Contrary to the well-known actin

ISSN Print 0013-7227 ISSN Online 1945-7170
Printed in U.S.A.

Received April 15, 2014. Accepted September 17, 2014.
First Published Online September 22, 2014

* X.K. and D.Y. contribute equally to this work.

Abbreviations: F-actin, filamentous actin; DMSO, dimethylsulfoxide; GLP-1, glucagon-like peptide-1-(7–36) amide; GSIS, glucose-stimulated insulin secretion; IBMX, 3-isobutyl-1-methylxanthine; KRB, Krebs-Ringer bicarbonate; MBS, myosin-binding subunit; MLC, myosin light chain; PKA, protein kinase A; ROCK, Rho-associated kinase.

cytoskeleton and its role in regulation of insulin secretion in normal β-cells, the importance of the actin cytoskeleton in β-cells in glucotoxicity, particularly its contribution to glucotoxicity-impaired GSIS, remains poorly understood.

The incretin hormone glucagon-like peptide-1-(7–36) amide (GLP-1) stimulates GSIS by elevating intracellular cAMP and subsequent activating protein kinase A (PKA) and an exchange protein directly activated by cAMP (exchange proteins activated by cAMP 2) (13) at physiological circumstances. We have found that GLP-1 potentiates GSIS in a PKA-dependent manner at glucotoxicity (14). However, the precise mechanism by which this is achieved remains unknown. In the present study, we demonstrate that chronic exposure of β-cells to high glucose increased stress fibers that were resistant to glucose-induced actin remodeling, which is particularly significant for impaired GSIS at glucotoxicity. GLP-1 rescued the glucotoxicity-induced alterations of the actin cytoskeleton and perturbations of GSIS via a PKA-dependent inhibition of the RhoA-Rho-associated kinase (ROCK) signaling pathway.

Materials and Methods

Animals, isolation of islets, and preparation and culture of β-cells

Female C57BL/6 mice (4–6 wk) were purchased from the Experimental Animal Centre of Guangdong Academy of Medical Science (Guangzhou, China). Mouse islets were isolated and cultured as described (14). The animal procedures were performed according to the Principles of Laboratory Animal Care and approved by the Shenzhen University Animal Care Committee.

Rat INS-1E cells were kindly provided by Professor Yong Liu from the Shanghai Institute for Nutritional Sciences of Chinese Academy of Sciences (Shanghai, China). The response of this cell line (14, 15) to glucose and incretin stimulations has been found to be similar to that of the glucose- and incretin-sensitive 832/3 β-cell line (16). INS-1E cells between passages 55 and 80 were cultured as previously reported (14).

For immunocytochemistry, the islets were dissociated into single cells using a Ca^{2+}-free solution. The resulting cell suspension was maintained in culture in DMEM containing 10% fetal bovine serum, 100 μM penicillin G, and 100 mg/ml streptomycin.

Immunocytochemistry and confocal microscopy

Primary β-cells and INS-1E cells plated onto glass coverslips were cultured in 5.5 mM glucose or 30 mM glucose medium for 72 hours. Cells were preincubated in Krebs-Ringer bicarbonate (KRB) buffer containing 10 μM cytochalasin B (Sigma) or 10 μM latrunculin B (Calbiochem) or 10 μM Y27632 (Selleck Chemicals) or 100 μM Rp-adenosine 3′,5′-cyclic monophosphorothioate triethylammonium salt or dimethylsulfoxide (DMSO) for 1 hour at 37°C, followed by stimulated with 2.8 mM glucose, 16.8 mM glucose alone or in the presence of 10 nM GLP-1 (Abcam), 10 μM forskolin, 1 mM 3-isobutyl-1-methylxanthine (IBMX; Sigma), 10 μM 6-Bnz-cAMP-AM (Biolog Life Science), and 100 μM Rp-cAMPS (Sigma) for the time as indicated, respectively. For actin labeling, cells were fixed with 3% paraformaldehyde and permeabilized in 0.1% Triton X-100. After blocking nonspecific sites, primary β-cells were incubated overnight at 4°C with a rabbit antiinsulin antibody (Cell Signaling; 1:75) and Alexa-Fluor546-labeled goat antirabbit (Invitrogen; 1:75) and treated with Alexa Fluor 488-phalloidin (Invitrogen) (17). INS-1E cells were directly incubated with Alexa Fluor 488-phalloidin after blocking. Images were obtained with a Zeiss 510 LSM confocal laser-scanning microscope.

Measurements of insulin secretion and content

Insulin release from mouse islets and INS-1E cells was assayed as published (14). Cells were preincubated in KRB buffer containing 10 μM cytochalasin B or 10 μM Y27632 or 1 μM jasplakinolide or 100 μM Rp-cAMPS or DMSO for 1 hour at 37°C. Then the cells were stimulated with 2.8 mM glucose, 16.8 mM glucose alone or in the presence of 10 nM GLP-1, 10 μM forskolin and 1 mM IBMX, 10 μM 6-Bnz-cAMP-AM, or 100 μM Rp-cAMPS or 1 μM jasplakinolide for the time as indicated, respectively. For insulin content assay, after incubation with 10 μM cytochalasin B for 1 hour, the whole-cell protein of islets and INS-1E cells was extracted. The insulin content was determined using an insulin ultrasensitive ELISA kit (ALPCO Diagnostics). Insulin levels (nanograms per milliliter) were normalized against total cellular protein content in milligrams.

Western blotting

After 72 hours' exposure to 5.5 mM glucose or 30 mM glucose medium, INS-1 cells were stimulated with 16.8 mM glucose alone or in the presence of 10 nM GLP-1 and 10 μM 6-Bnz-cAMP-AM for the time as indicated, respectively. Proteins resolved by SDS-PAGE were immunoblotted as previously described (14). The primary antibodies purchased from Santa Cruz Biotechnology were as follows: polyclonal rabbit antiactin, polyclonal rabbit anti-β-tubulin, and monoclonal mouse anti-RhoA. The primary antibodies purchased from Cell Signaling were as follows: monoclonal rabbit antiglyceraldehyde-3-phosphate dehydrogenase, polyclonal rabbit anti-p-myosin-binding subunit (MBS), polyclonal rabbit anti-MBS, polyclonal rabbit anti-p-myosin light chain (MLC), and polyclonal rabbit anti-MLC. The secondary antibodies were horseradish-peroxidase-conjugated goat antimouse (Abcam) and goat antirabbit (Sigma-Aldrich).

F-actin/G-actin assay

INS-1E cells were cultured in the medium containing 5.5 mM or 30 mM glucose for 72 hours, followed by exposure to KRB buffer containing 10 μM cytochalasin B or 10 μM latrunculin B or 10 μM Y27632 or 100 μM Rp-cAMPS or DMSO for 1 hour at 37°C. The cells were stimulated with 16.8 mM glucose alone or in the presence of 10 nM GLP-1, 10 μM forskolin and 1 mM IBMX, 10 μM 6-Bnz-cAMP-AM, and 100 μM Rp-cAMPS for the time as indicated. The cells were harvested and the level of F- and G-actin in cell extracts was assessed with G-actin/F-actin in vivo assay kit (Cytoskeleton) according to the manufacturer's instructions.

Measurement of the activity of RhoA

After 72 hours of culture in the medium containing 5.5 mM or 30 mM glucose, INS-1E cells were preincubated with KRB buffer for 1 hour and then were exposed to KRB buffer contain-

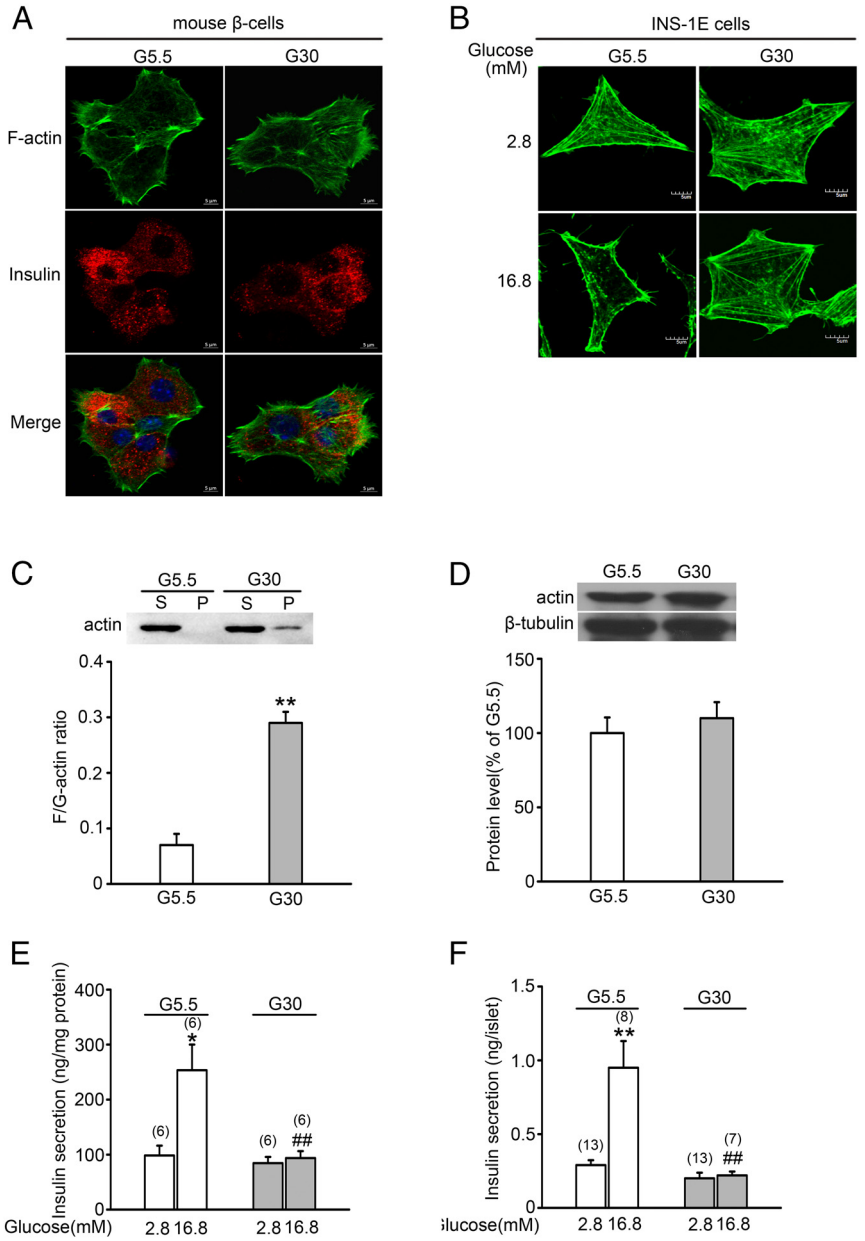

Figure 1. Chronic culture at high glucose increases stress fiber and diminishes GSIS. A, Primary β-cells at G5.5 or G30 for 72 hours. Confocal microscopy images showing actin cytoskeleton (green, top panels) and insulin (red, middle panels) and merged of the two (bottom panels). Scale bars represent 5 μm. B, Similar to panel A but the images showing actin cytoskeleton of INS-1E cells after stimulation with 2.8 mM glucose (top panels) or 16.8 mM glucose (bottom panels), respectively. C, A representative immunoblot for F-actin to G-actin ratio are shown on the top. Supernatant (S) and pellet (P) fractions contain G-actin and F-actin, respectively. The relative intensities of the F-actin and G-actin were quantified and expressed as a ratio. Data are means ± SEM of three experiments each. **, $P < .01$. D, A representative immunoblot is shown on the top. β-Tubulin was used as the control. Values are expressed as percentage of protein abundance at G5.5. Data are means ± SEM of five experiments each. E and F, Insulin secretion was stimulated in INS-1 cells (E) or mouse islets (F) with 2.8 and 16.8 mM glucose for 10 minutes (E) or 1 hour (F). Values were normalized for total protein (E) or represented the amount of secretion per islet (F). Data are means ± SEM. *, $P < .05$; **, $P < .01$ vs 2.8 mM glucose; ##, $P < .01$ vs 16.8 mM glucose at G5.5.

ing 16.8 mM glucose for 10 minutes and harvested. Quantification of active (GTP bound) RhoA in cell extracts was assessed using a G-LISA RhoA activation assay biochemistry kit (Cytoskeleton) according to the manufacturer's instructions.

Statistics

Data are presented as mean ± SEM for the indicated number of experiments. Statistical significance was evaluated using the independent *t* test. Data were considered significant at a value of $P < .05$.

Results

Glucotoxicity increases stress fibers and abolishes GSIS

We and others have used primary β-cells and INS-1E cells as the model for studying glucotoxicity by culturing the cells in 30 mM glucose (G30) for 72 hours (4, 14). In basal (2.8 mM glucose) conditions, phalloidin staining for F-actin showed that both primary β-cells (Figure 1A) and INS-1E cells (Figure 1B) at G30 were rich in long stress fibers, as compared with cells in 5.5 mM glucose (G5.5). The glucotoxicity-induced increase in stress fibers was supported by the analysis of the F-actin to G-actin ratio that was 30%:70% at G30, as compared with 7%:93% at G5.5 (Figure 1C); the latter is comparable with the previous observation (10%:90%) in MIN6 cells (18). Note that the actin contents at G30 were comparable with that at G5.5 (Figure 1D). Thus, chronic exposure to high glucose results in increased formation of stress fibers, rather than a general increase of cellular actin content. Notably, stimulation with 16.8 mM glucose for 10 minutes had little effect on the actin cytoskeleton at G30, whereas at G5.5 glucose stimulation induced F-actin depolymerization (Figure 1B). Indeed, the majority (108 of 143) of cells at G30 were resistant to glucose-induced actin remodeling, in contrast to approximately 87% (109 of 125) of cells at G5.5 displaying glucose-stimulated actin depolymerization.

We next proceeded to determine the effects of glucotoxicity on GSIS. As shown in Figure 1E, administration of 16.8 mM glucose produced an approximately 3-fold increase of insulin secretion at G5.5,

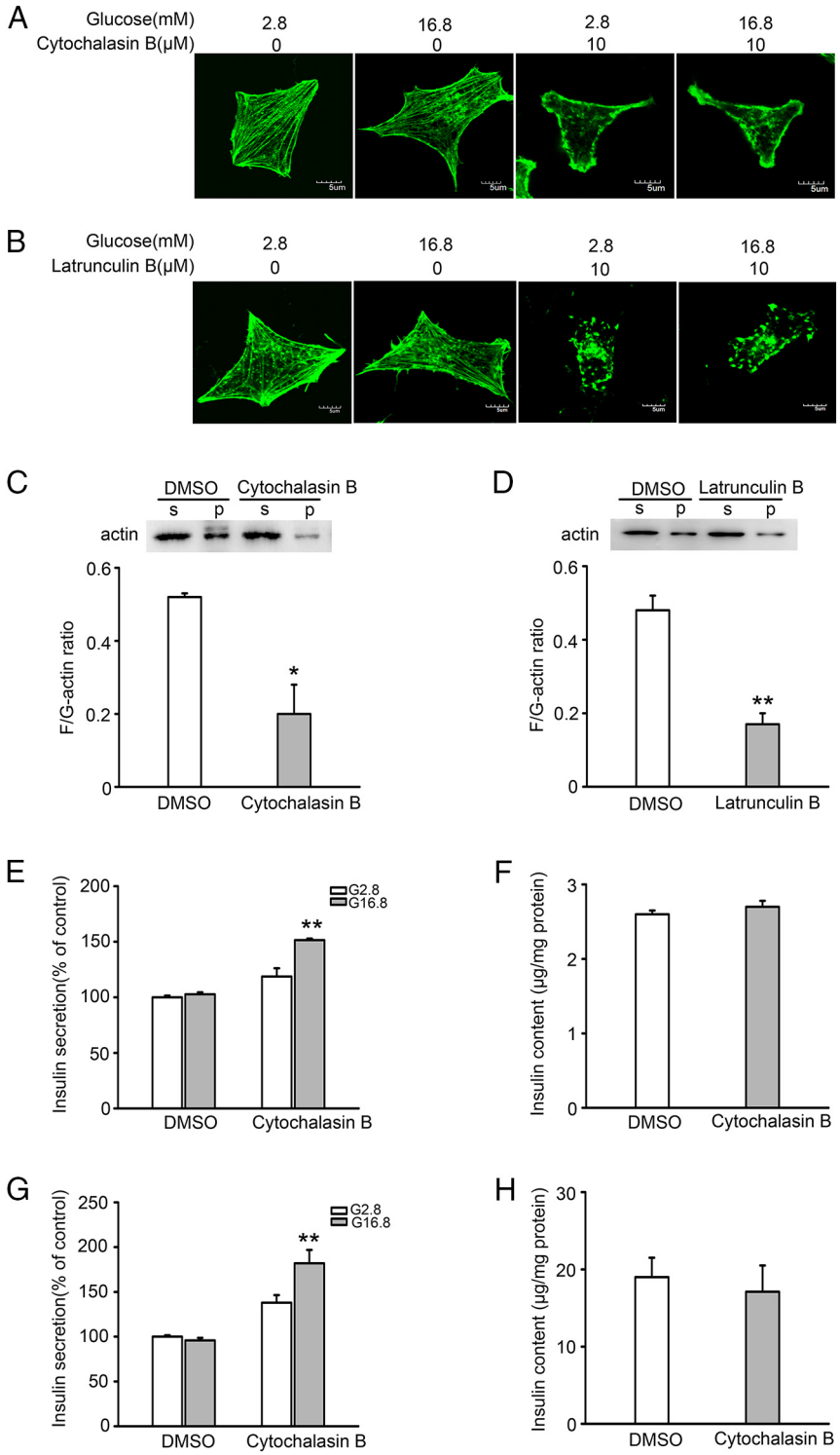

Figure 2. Effects of actin depolymerizing agents on GSIS. A and B, Phalloidin-staining actin cytoskeleton upon stimulation with 2.8 mM glucose or 16.8 mM glucose in the absence or presence of cytochalasin B (A) and latrunculin B (B), respectively. Scale bars represent 5 μm. C and D, Same as Figure 1 (C) but F-actin to G-actin ratio was determined by pretreatment with DMSO or cytochalasin B (C) or latrunculin B (D) for 1 hour. Data are means ± SEM of three (C) or four (D) experiments each. **, $P < .01$. E and G, Insulin secretion was assayed in INS-1E cells (E) or mouse islets (G) by pretreatment with DMSO or cytochalasin B for 1 hour followed by stimulation with 2.8 mM or 16.8 mM glucose. Data are means ± SEM of five (E) or three (G) experiments each. **, $P < .01$ vs 2.8 mM glucose. F and H, Insulin content of INS-1 cells (F) or mouse islets (H) was assayed with or without cytochalasin B. Data are means ± SEM of five (F) or three (H) experiments each.

whereas glucose stimulation caused little increase of insulin secretion at G30, as reported previously (4, 14). We also sought to determine whether these findings could be replicated in mouse islets. Treatment with 16.8 mM glucose resulted in an approximately 3.3-fold increase of insulin secretion at G5.5, whereas GSIS was abolished at G30 (Figure 1F). However, basal insulin secretion at G30 was comparable with that at G5.5 (Figure 1, E and F), as reported previously (14).

Actin depolymerization by cytochalasin B or latrunculin B restores GSIS at glucotoxicity

To explore whether glucotoxicity-diminished GSIS observed in Figure 1, E and F, could be attributed to the impact of increased stress fibers, we preincubated INS-1E cells at G30 without or with cytochalasin B (10 μM), an F-actin-disrupting agent (Figure 2A), or a more selective G-actin-binding and sequestering agent, latrunculin B (10 μM) (Figure 2B), for 1 hour before 10 minutes of stimulation with 2.8 or 16.8 mM glucose. Pretreatment with these actin depolymerising agents disrupted the actin cytoskeleton (Figure 2, A and B), converting the F-actin to G-actin ratio from 52%:48% to 20%:80% for cytochalasin B (Figure 2C) or to 17%:83% for latrunculin B (Figure 2D). Actin depolymerization resulted in an increase of approximately 1.9-fold ($P < .01$) or approximately 1.6-fold ($P < .01$) of GSIS, respectively, in cytochalasin B-pretreated INS-1E cells (Figure 2E) or islets (Figure 2G) at G30. Similar insulinotropic effect was observed by pretreatment with latrunculin B (Supplemental Figures 1B and 2A). Notably, the increase in GSIS by these actin-depolymerizing agents was not accompanied by changes in insulin content (Figure 2, F and H; Supplemental Figures 1C and 2B), as compared with control DMSO-treated cells.

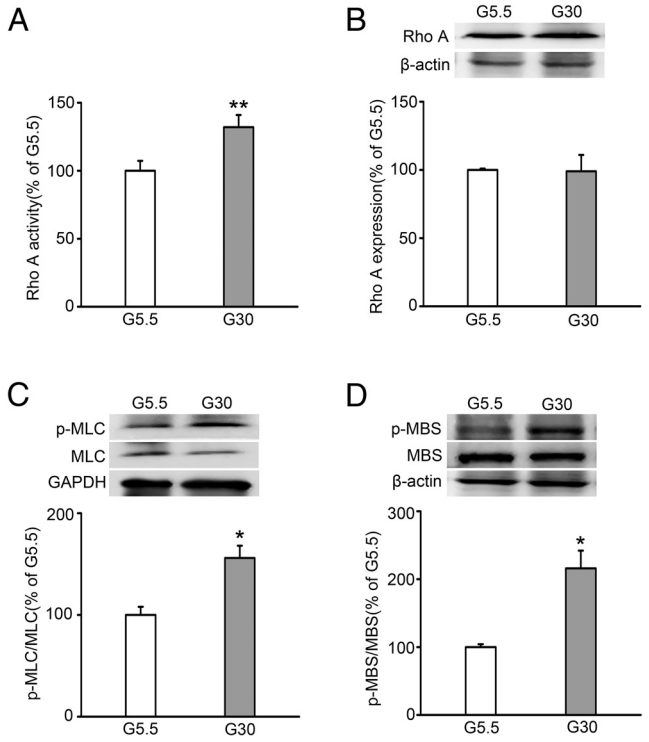

Figure 3. Effects of glucotoxicity on RhoA and ROCK activity. A, INS-1E cells cultured at G5.5 and G30 for 72 hours. RhoA activity was measured with a RhoA assay kit and expressed as a percentage of G5.5. Data are expressed as means ± SEM of four experiments. **, $P < .01$. B, A representative immunoblot for RhoA protein expression is shown on the top. β-Actin was used as the control. Intensities were quantified and normalized against the level of β-actin and expressed as the percentage of protein abundance at G5.5. Data are means ± SEM of three experiments. C and D, A representative immunoblot is shown on the top. Glyceraldehyde-3-phosphate dehydrogenase (GAPDH) (C) or β-actin (D) was used as the control. The relative intensities of p-MLC and total MLC protein (C) or p-MBS and total MBS protein (D) were quantified and expressed as a ratio. Ratios were normalized to cells at G5.5. Data are means ± SEM of three (C) or four (D) experiments. *, $P < .05$.

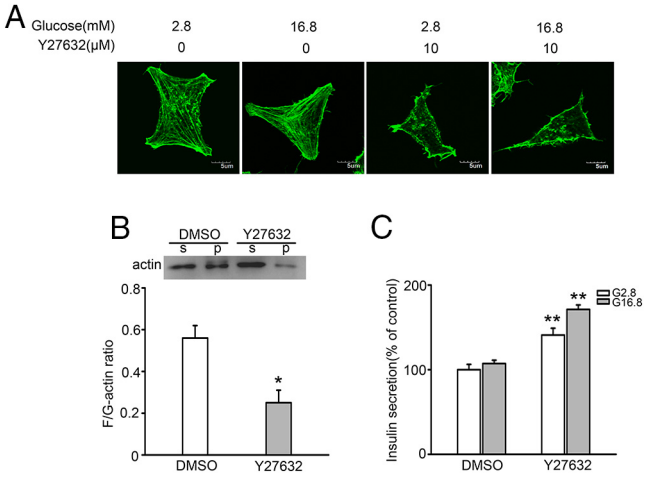

Figure 4. Impact of the inhibition of ROCK on F-actin cytoskeleton and GSIS. A, Phalloidin-staining actin cytoskeleton of INS-1E cells at G30 after stimulation with 2.8 mM glucose or 16.8 mM glucose in the absence or presence of Y-27632. Scale bars represent 5 μm. B, Same as Figure 1 (C) but F-actin to G-actin ratio was determined by pretreatment with DMSO or Y-27632 for 1 hour. Data are means ± SEM of four experiments each. *, $P < .05$. C, Insulin secretion was assayed by pretreatment with DMSO or 10 μM Y-27632 for 1 hour followed by stimulation with 2.8 mM or 16.8 mM glucose. Data are means ± SEM of three experiments each. **, $P < .01$ vs 16.8 mM glucose in DMSO.

Glucotoxicity increased RhoA and ROCK activities

It is known that RhoA, a member of the Ras superfamily of small GTPases, and its effector ROCK are the key regulators of stress fiber formation (19). Therefore, we explored whether chronic high glucose promoted stress fiber formation by stimulating RhoA and ROCK activities. We first examined the effects of high glucose on the activities of RhoA by incubating INS-1E cells at either G5.5 or G30 for 72 hours. As shown in Figure 3A and Supplemental Figure 3, cells at G30 displayed a significantly higher RhoA activity as compared with cells at G5.5, whereas RhoA expression at G30 was similar to that at G5.5 (Figure 3B). As the key downstream effector of RhoA, ROCK is activated by RhoA binding and causes stress fiber formation (20) and thereby inhibits insulin secretion (21). We next examined ROCK activity by measuring phosphorylated protein levels of its substrates, MLC and the regulatory subunit of myosin light chain phosphatase, MBS (22). As shown in Figure 3, C and D, cells at G30 displayed significantly higher phosphorylated p-MLC/MLC and p-MBS/MBS compared with cells at G5.5, respectively. Although chronic exposure to high glucose increased the pMLC, the total MLC remained largely unchanged at the protein level (Supplemental Figure 4).

We next explored whether glucotoxicity-induced RhoA/ROCK activation plays a role in stress fiber formation and inhibition of GSIS at glucotoxicity. Cells cultured at G30 for 72 hours were stimulated with 2.8 mM or 16.8 mM glucose for 10 minutes in the absence or presence of 10 μM Y27632, a ROCK-specific inhibitor. As shown in Figure 4A, treatment with Y27632 resulted in a marked actin depolymerization (Figure 4A), accompanied by the reduction of the F-actin to G-actin ratio (Figure 4B) and an approximately 1.6-fold increase ($P < .01$) of GSIS (Figure 4C).

GLP-1 is capable of depolymerizing stress fiber-rich actin cytoskeleton

To test whether GLP-1 could affect glucotoxicity-increased stress fibers, we incubated primary β-cells (Figure 5A) and INS-1E cells (Figure 5B) at G30 for 72 hours and treated with 2.8 mM glucose or 16.8 mM glucose in the absence or presence of 10 nM GLP-1 for 10 minutes. As shown in Figure 5, A and B, primary β-cells (Figure 5A) and INS-1E cells (Figure 5B) retained a stress fiber-rich actin cytoskeleton upon glucose stimulation, whereas treatment with GLP-1 resulted in actin depolymeriza-

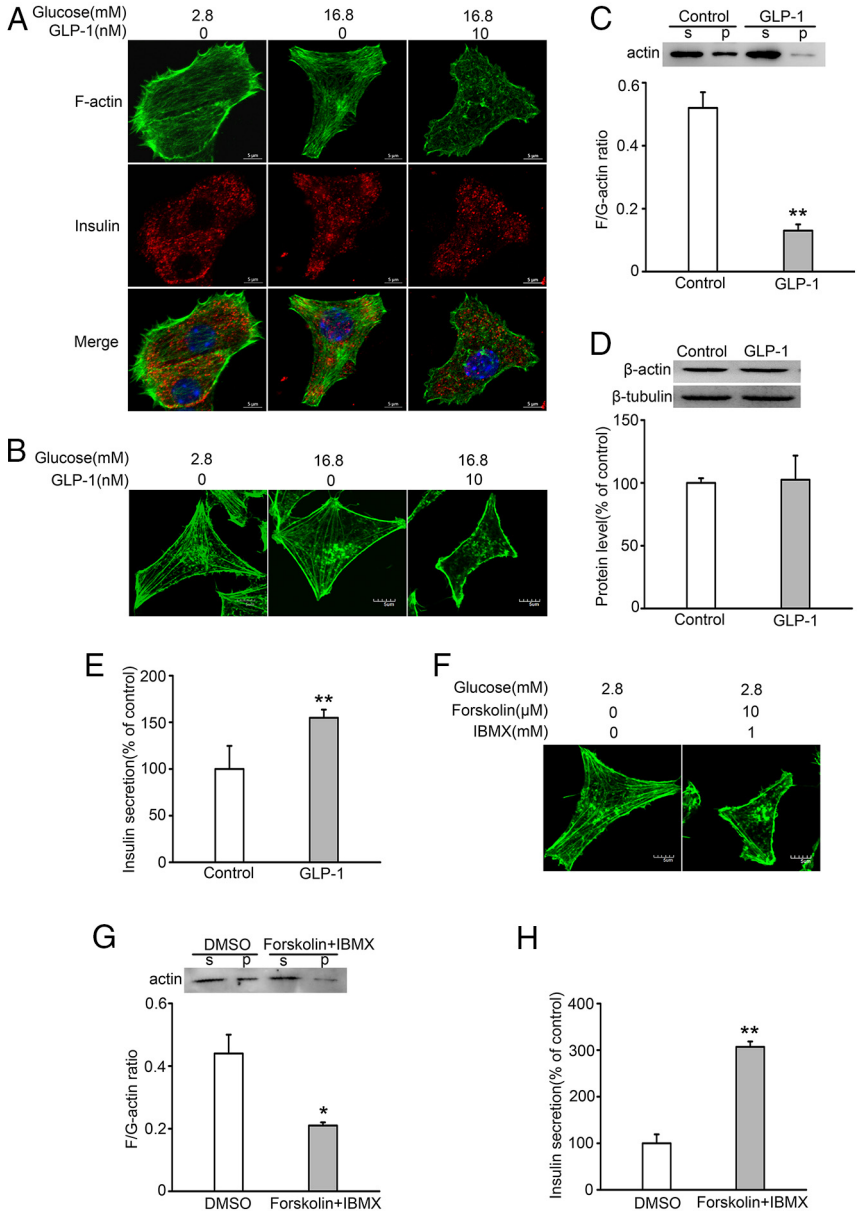

Figure 5. Effects of GLP-1 on F-actin remodeling and GSIS. A, Primary β-cells cultured at G30 for 72 hours. Confocal microscopy images showing actin cytoskeleton (green, top panels) and insulin (red, middle panels) and merged of the two (bottom panels) after stimulation with 2.8 mM glucose or 16.8 mM glucose without or with GLP-1, respectively. Scale bars represent 5 μm. B and F, Same as (panel A but actin cytoskeleton of INS-1E in the absence or presence of GLP-1 (B) or forskolin and IBMX (F). Scale bars represent 5 μm. C and G, Same as Figure 1 (C) but F-actin to G-actin ratio was determined without or with treatment of GLP-1 (C) or forskolin and IBMX (G) for 10 minutes. Data are means ± SEM of four (C) or three (G) experiments each. *, $P < .05$; **, $P < .01$. D, Same as Figure 1 (D), but the actin protein level was determined without or with treatment with GLP-1 for 10 minutes. Data are means ± SEM of three experiments each. E and H, Insulin secretion was stimulated with 16.8 mM glucose in the absence or presence of GLP-1 (E) or forskolin and IBMX (H) for 10 minutes. Data are means ± SEM of three (E) or six (H) experiments. **, $P < .01$.

tion, converting the F-actin to G-actin ratio from 52%:48% to 13%:87% (Figure 5C). The cellular morphology of GLP-1-treated cells was comparable with that of the ROCK inhibitor-treated cells (Figure 4A). In addition, GLP-1 had no effect on actin content (Figure 5D). The effect of GLP-1 was mimicked by the cAMP-increasing agents forskolin and IBMX (Figure 5, F and G). Moreover, actin depolymerization by GLP-1 or forskolin and IBMX was accompanied by potentiated GSIS (Figure 5, E and H).

GLP-1 inhibits ROCK activity and restores GSIS via a PKA-dependent manner

Figure 5 (A, B, and E) shows the effect of GLP-1 on actin depolymerization, and GSIS was the same as that observed with the ROCK inhibitor in Figure 4, A and C, suggesting that GLP-1 could exert its effects via suppressing ROCK activity. To test this possibility, INS-1E cells cultured at G30 for 72 hours were treated with or without 10 nM GLP-1 for 15 minutes, and the ROCK activity was determined by measuring p-MBS and total MBS or p-MLC and total MLC. As shown in Figure 6, A and B, treatment of cells with GLP-1 significantly reduced the levels of phosphorylated-MBS and phosphorylated-MLC, whereas GLP-1 had little effect on the expression of the total MLC (Supplemental Figure 5).

Because GLP-1 restores glucotoxicity-blunted GSIS mainly via activation of PKA (14), we therefore explored the PKA-dependent effects of GLP-1 on the actin cytoskeleton and its importance for GSIS in glucotoxicity. INS-1E cells cultured at G30 for 72 hours were stimulated with 16.8 mM glucose alone or 10 μM 6-Bnz-cAMP-AM (a PKA agonist) or 10 nM GLP-1 or a combination of 10 nM GLP-1 and 100 μM Rp-cAMPS (a PKA inhibitor) for 10 minutes. As shown in Figure 7A, the actin cytoskeleton remained unchanged after glucose stimulation, whereas treatment with GLP-1 or 6-Bnz-cAMP-AM resulted in substantial actin depolymerization, converting the F-actin to G-actin ratio from 55%:45% to 13%:87% or to 24%:76%, respectively (Figure 7B), Notably, GLP-1 and 6-Bnz-cAMP-AM had no effects on cellular actin con-

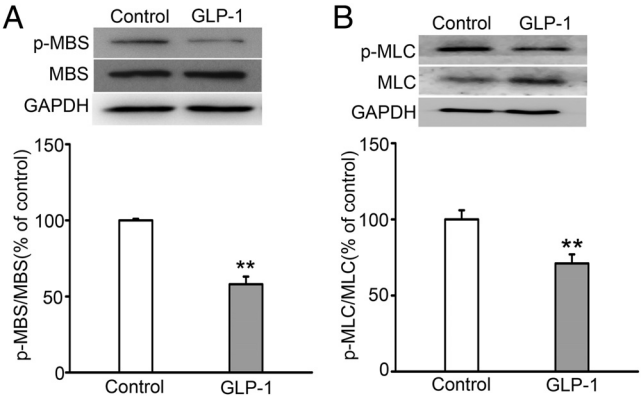

Figure 6. Effect of GLP-1 on glucotoxicity-induced ROCK activation. A and B, The graph is similar to Figure 3, C and D, but intensities of p-MBS and total MBS protein (A) or the p-MLC and total MLC protein (B) were determined in the absence or presence of GLP-1. Ratios were normalized to in the absence of GLP-1. Data are means ± SEM of seven (A) or five (B) experiments. GAPDH, glyceraldehyde-3-phosphate dehydrogenase. **, $P < .01$.

tent (Figures 5D and 7C). Actin depolymerization by GLP-1 or 6-Bnz-cAMP-AM resulted in an approximately 2.5-fold or an approximately 2.3-fold increase of GSIS (Figure 7, D and E). The link of GLP-1-induced the depolymerization of stress fibers and potentiation of GSIS was reinforced by the experiments performed in cells at G30 that were treated with 10 nM GLP-1 or 10 μM 6-Bnz-cAMP for 10 minutes, in the absence or presence of jasplakinolide, an F-actin polymerizing and stabilizing agent (11, 12, 23). As shown in Figure 7, D and E, the stimulatory effect of either GLP-1 or 6-Bnz-cAMP-AM on GSIS was largely blocked by jasplakinolide, confirming that GLP-1 potentiated GSIS, at least partly, via disassembling F-actin. Moreover, the effect of GLP-1 on actin cytoskeleton (Figure 7, A and B) and GSIS (Figure 7D) was sensitive to the PKA inhibitor Rp-cAMPS.

The PKA-mediated effect of GLP-1 was further evidenced by the observation that GLP-1 was unable to provide additional stimulation of GSIS in the presence of 10 μM 6-Bnz-cAMP-AM (Figure 7E), confirming that PKA activation is responsible for the insulinotropic action of GLP-1 at glucotoxicity. In addition, treatment with 6-Bnz-cAMP-AM suppressed ROCK activity (Figure 7F), resembling the effect of GLP-1. Together this series of complementary experiments indicate that the PKA-mediated suppression of ROCK signaling and subsequent F-actin depolymerization contributes to GLP-1-potentiated GSIS in glucotoxicity.

Discussion

It has been suggested that glucotoxicity-impaired GSIS plays a crucial role in β-cell dysfunction in type 2 diabetes. Although glucotoxicity induced a certain rate of apoptosis contributes to impaired insulin secretion, we have demonstrated here, for the first time, that the formation of the stress fiber-rich actin cytoskeleton is also involved in glucotoxicity-diminished GSIS. This abnormal actin cytoskeleton was resistant to glucose-stimulated remodeling. These findings were obtained in both primary β-cells and INS-1E cells. We further show that GLP-1 and cAMP-increasing agents reversed glucotoxicity-inhibited GSIS by depolymerising the F-actin cytoskeleton. The GLP-1/cAMP-mediated restoration of glucotoxicity-inhibited GSIS was accounted for by a PKA-dependent inhibition of the RhoA-ROCK signaling pathway in glucotoxic β-cells. Finally, several variants of *RHOA* were found to be associated with metabolic traits in humans, suggesting relevance for human metabolic disease.

Our results show that β-cells at high glucose developed stress fiber-rich actin cytoskeleton, which was resistant to glucose-induced actin remodeling. By contrast, β-cells at low glucose exhibited more curved cortical actin filaments and glucose-stimulated actin depolymerization. It is worthy to note that glucose-insensitive C3 subline of MIN6 cells was rich in stress fibers, which led to secretory deficiency upon glucose stimulation (17). Our data also argue that the increased amount of stress fibers would be attributed to actin polymerization state, rather than a general increase of cellular F-actin content (Figure 1D). Additionally, an increase of F-actin stress fibers at G30 can not be attributed to osmotic effects, given that treatment with 5.5 mM glucose + 24.5 mM D-mannitol (the same osmolarity as that at G30) failed to induce alteration of actin cytoskeleton and insulin secretion (Supplemental Figure 6, A–C), confirming that hyperglycemia per se rather than hyperosmolarity induced the increase of stress fibers and diminished GSIS.

Our data show that glucotoxicity is associated with the formation of stress fiber-rich actin cytoskeleton in pancreatic β-cells. This is likely to impair the secretory response to glucose stimulation (14), given that actin depolymerization is important for exocytosis of insulin-containing granules (24). Based on these observations and coupled with fact that stress fibers reduce GSIS in normal β-cells (17), it is justifiable to conclude that the abnormal actin cytoskeleton is at least partly responsible for glucotoxicity-diminished GSIS. Two observations corroborate this concept. First, β-cells at glucotoxicity retained the stress fiber-rich actin cytoskeleton and displayed no response to stimulation with 16.8 mM glucose, whereas β-cells at low glucose exhibited glucose-stimulated actin depolymerization and insulin secretion. Second, depolymerising agents, either cytochalasin B or latrunculin B, ie, two distinct types of F-actin depolymerizing agents, disrupted the rigid actin cytoskeleton and restored glucotoxicity-diminished GSIS. More mechanistic insight is needed to prove the causal relation between generation of

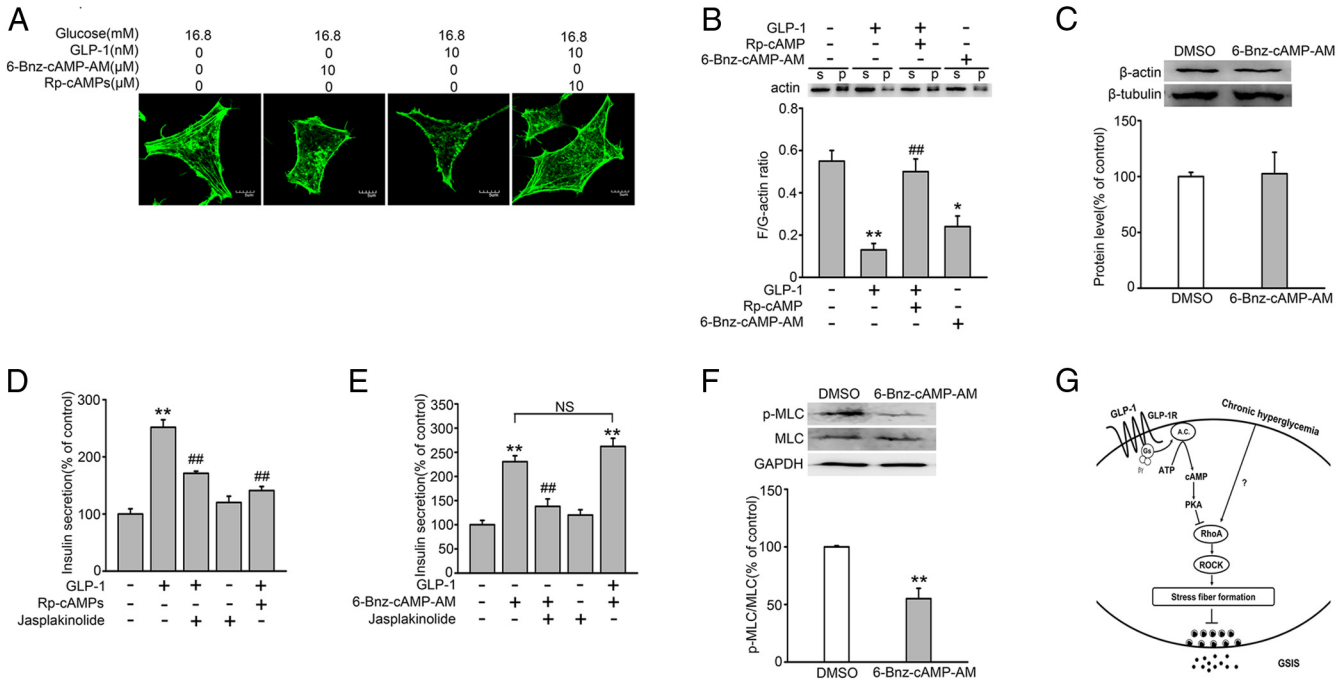

Figure 7. PKA-dependent effects of GLP-1 on F-actin remodeling and GSIS. A, Phalloidin-staining actin cytoskeleton of INS-1E cells in the presence of 16.8 mM glucose alone, the addition of 6-Bnz-cAMP-AM, or GLP-1, or simultaneously the addition of GLP-1 and Rp-cAMPS, respectively. Scale bars represent 5 μm. B, Same as Figure 1 (C) but F-actin to G-actin ratio was determined in the absence or presence of GLP-1, or 6-Bnz-cAMP-AM, or the simultaneous presence of GLP-1 and Rp-cAMPS, for 10 minutes. Data are means ± SEM of three experiments each. *, $P < .05$; **, $P < .01$ vs control; ##, $P < .01$ vs GLP-1. C, Same as Figure 1 (D), but the actin protein level was determined with DMSO (control) or 6-Bnz-cAMP-AM. Data are means ± SEM of three experiments each. D, Insulin secretion was assayed with stimulation by 16.8 mM glucose alone, the addition of GLP-1, or jasplakinolide, the simultaneous addition of GLP-1 and Rp-cAMPS, or GLP-1 and jasplakinolide, respectively, for 10 minutes. Data are means ± SEM of five experiments each. **, $P < .01$ vs control; ##, $P < .01$ vs GLP-1. E, Same as panel D, but insulin secretion was assayed in cells stimulated by 16.8 mM glucose alone, the addition of 6-Bnz-cAMP-AM or jasplakinolide, or the simultaneous addition of 6-Bnz-cAMP-AM and GLP-1, or GLP-1 and jasplakinolide, respectively, for 10 minutes. Data are means ± SEM of five experiments each. **, $P < .01$ vs control; ##, $P < .01$ vs 6-Bnz-cAMP-AM. F, Same as Figure 3 (C) but p-MLC and total MLC protein was determined with DMSO or 6-Bnz-cAMP-AM. Data are means ± SEM of six experiments. **, $P < .01$. G, Schematic of a proposed model for of GLP-1-linked pathway potentiates GSIS via depolymerizing F-actin at glucotoxicity. See text for details. GAPDH, glyceraldehyde-3-phosphate dehydrogenase.

stress fibers and decreased secretory response of pancreatic β-cells.

It is known that the RhoA/ROCK pathway is the major regulator of stress fiber formation (19) and is responsible for the stabilization of the actin cytoskeleton and inhibition of insulin secretion at physiological conditions (21). Given that chronic high glucose stimulates the activities of RhoA and ROCK, we hypothesized that glucotoxicity-increased RhoA/ROCK activity would contribute to the increased stress fibers in β-cells. This conclusion is reinforced by the experiments performed in INS-1E cells at G30 with treatment with the ROCK inhibitor Y27632. This resulted in disruption of the actin cytoskeleton and restored glucotoxicity-diminished GSIS. Currently we have not resolved how glucotoxic conditions activate RhoA/ROCK. It is generally agreed that signals received by cell surface receptors, via messengers such as cytokines, growth factors, and hormones, are transmitted to the Rho family (25, 26). Consistently, stimulation of tyrosine kinase and G protein-coupled receptors activates RhoA, which interacts with the Rho-binding domain of ROCK and results in the activation of ROCK (27). Thus, elucidation of whether tyrosine kinase and G protein-coupled receptors implicated glucotoxicity-induced activation of RhoA warrants further investigations.

The ability of GLP-1 to stimulate insulin secretion has been well established (13, 28). However, the insulinotropic action of GLP-1 under glucotoxic conditions has been rarely documented. We have reported recently that GLP-1 potentiates GSIS in a PKA-dependent manner during glucotoxicity (14). In the present study, we demonstrate that GLP-1 potentiates glucotoxicity-diminished GSIS by depolymerizing actin cytoskeleton (Figure 5, A–C and E), an effect that is mimicked by forskolin and IBMX (Figure 5, F and H). The cAMP-PKA-mediated effects of GLP-1 on actin depolymerization and GSIS observed at glucotoxic conditions are supported by four lines of evidence. First, GLP-1 failed to induce actin depolymerization and stimulate GSIS in the presence of MDL-12330A, a specific adenylyl cyclase inhibitor (Supplemental Figure 7). Second, GLP-1 lost its ability to depolymerize actin cytoskeleton (Figure 7, A and B) and potentiate GSIS (Fig-

ure 7D) in the presence of Rp-cAMPS. Third, GLP-1 failed to produce additional stimulation of GSIS when PKA was activated by 6-Bnz-cAMP-AM (Figure 7E). Fourth, treatment of β-cells with 6-Bnz-cAMP-AM mimicked the effects of GLP-1 on actin depolymerization (Figure 7, A and B), GSIS (Figure 7E), and inhibition of ROCK (Figure 7F).

It may seem surprising that whereas our data indicate that cAMP-elevating agents are capable of depolymerizating actin cytoskeleton, experiments on Min6 cells treated with the cAMP phosphodiesterase inhibitor IBMX suggest failure of cAMP to induce actin depolymerization (17). This discrepancy would not be so unexpected, given that those experiments were performed by the application of 1 mM IBMX alone and without extracellular glucose, whereas our observations were obtained by the application of 10 μM forskolin and 1 mM IBMX together and under more physiological basal conditions (2.8 mM glucose). It is important to note that extracellular glucose is required for cAMP-dependent effects in pancreatic β-cells (29). Another possible explanation is that cAMP-induced actin depolyermization would be operational when intracellular cAMP concentrations are high enough to activate PKA, given the PKA-dependent effects are cAMP dependent with a dissociation constant of 6 μM in pancreatic β-cells (28).

The ability of GLP-1 to depolymerize the actin cytoskeleton is further confirmed by the observations that treatment of INS-1E cells with GLP-1 or 6-Bnz-cAMP-AM suppressed glucotoxicity-increased ROCK activities. The effects of GLP-1 and 6-Bnz-cAMP-AM were reminiscent of those observed in endothelial cells (25) and mouse lymphoid cell line (26), which showed that cAMP inhibited both thrombin- or chemoattractant-induced RhoA activation and translocation through activation of PKA. Based on the present findings and those published (4, 14), we outline a hypothetical model that explains our findings (Figure 7G). Thus, chronic exposure of β-cells to high glucose would result in RhoA activation and subsequent ROCK activation. Activated ROCK phosphorylates MLC and inhibits MLCP activity (22), thereby coordinately increase the phosphorylation of MLC and result in stress fiber formation (30).

Importantly, the present study shows that GLP-1 suppressed glucotoxicity-stimulated RhoA/ROCK activation in a PKA-dependent manner. Indeed, it has been found that PKA inhibits RhoA activation by direct phosphorylation of the COOH terminus at Ser188, allowing the GTP-bound form of RhoA to be complexed with guanine nucleotide dissociation inhibitor (31). Nonetheless, inhibition of RhoA/ROCK activation by PKA would favor depolymerization of stress fiber-rich actin cytoskeleton, given the central role of RhoA/ROCK in formation and stabilization of stress fibers (32). Actin depolymerization in turn facilitates exocytosis of insulin-containing granules. Taken together, our findings suggest that glucotoxicity-altered actin cytoskeleton organization and remodeling at least partly account for the impaired GSIS caused by hyperglycemic conditions.

GLP-1 can antagonize the glucotoxic inhibition of GSIS via suppressing RhoA/ROCK signaling and F-actin depolymerization. This is interesting, given the fact that we found that several variants of *RHOA* were significantly associated with elevated fasting insulin and homeostasis model assessment index of insulin resistance, both parameters reflecting insulin resistance. Whether the single-nucleotide polymorphisms confer altered expression of *RHOA* is not resolved, but some are located in the genomic region of regulatory elements (Supplemental Table 1). In addition, we have previously found that under lipotoxic conditions, expression of RHOA mRNA is elevated in clonal INS-1-derived cells (mean of Z-score 1.7; q value <0.05) (33). This could potentially have contributed to the impairment of GSIS observed, in view of the negative effects exerted in β-cells by RHOA in the current study. The results in our study suggest a novel cellular function of GLP-1.

Acknowledgments

We thank Dr Hongbo Chen (Graduate School of Shenzhen Tsinghua University) for kind help in the immunofluorescence, Dr Qingning Su (Shenzhen University Health Science Center) for providing technical assistance in confocal microscopy.

Address all correspondence and requests for reprints to: Professor Xiaosong Ma, PhD, Diabetes Centre, School of Medicine, Nanhai Avenue 3688, Shenzhen University, Shenzhen 518060, China. E-mail: xsma@szu.edu.cn.

This work was supported by grants from the National Nature Science Foundation of China (to X.M.) and the Shenzhen Scientific and Innovative Committee. This work was also supported by the China Postdoctoral Science Foundation (to X.K.). J.S. and H.M. were supported by the Swedish Research Council.

Disclosure Summary: The authors have nothing to disclose.

References

1. **Robertson RP, Harmon J, Tran PO, Poitout V.** β-Cell glucose toxicity, lipotoxicity, and chronic oxidative stress in type 2 diabetes. *Diabetes*. 2004;53(suppl 1):S119–S124.
2. **Nyblom HK, Thorn K, Ahmed M, Bergsten P.** Mitochondrial protein patterns correlating with impaired insulin secretion from INS-1E cells exposed to elevated glucose concentrations. *Proteomics*. 2006;6(19):5193–5198.
3. **Marshak S, Leibowitz G, Bertuzzi F, et al.** Impaired beta-cell functions induced by chronic exposure of cultured human pancreatic islets to high glucose. *Diabetes*. 1999;48(6):1230–1236.
4. **Dubois M, Vacher P, Roger B, et al.** Glucotoxicity inhibits late steps of insulin exocytosis. *Endocrinology*. 2007;148(4):1605–1614.

5. **Rorsman P, Renstrom E.** Insulin granule dynamics in pancreatic β cells. *Diabetologia*. 2003;46(8):1029–1045.
6. **Wang Z, Thurmond DC.** Mechanisms of biphasic insulin-granule exocytosis—roles of the cytoskeleton, small GTPases and SNARE proteins. *J Cell Sci*. 2009;122(Pt 7):893–903.
7. **Orci L, Gabbay KH, Malaisse WJ.** Pancreatic β-cell web: its possible role in insulin secretion. *Science*. 1972;175(4026):1128–1130.
8. **Wang JL, Easom RA, Hughes JH, McDaniel ML.** Evidence for a role of microfilaments in insulin release from purified β-cells. *Biochem Biophys Res Commun*. 1990;171(1):424–430.
9. **Thurmond DC, Gonelle-Gispert C, Furukawa M, Halban PA, Pessin JE.** Glucose-stimulated insulin secretion is coupled to the interaction of actin with the t-SNARE (target membrane soluble N-ethylmaleimide-sensitive factor attachment protein receptor protein) complex. *Mol Endocrinol*. 2003;17(4):732–742.
10. **Jijakli H, Zhang HX, Dura E, Ramirez R, Sener A, Malaisse WJ.** Effects of cytochalasin B and D upon insulin release and pancreatic islet cell metabolism. *Int J Mol Med*. 2002;9(2):165–172.
11. **Lawrence JT, Birnbaum MJ.** ADP-ribosylation factor 6 regulates insulin secretion through plasma membrane phosphatidylinositol 4,5-bisphosphate. *Proc Natl Acad Sci USA*. 2003;100(23):13320–13325.
12. **Nevins AK, Thurmond DC.** Glucose regulates the cortical actin network through modulation of Cdc42 cycling to stimulate insulin secretion. *Am J Physiol Cell Physiol*. 2003;285(3):C698–C710.
13. **Holst JJ.** The physiology of glucagon-like peptide 1. *Physiol Rev*. 2007;87(4):1409–1439.
14. **Luo G, Kong X, Lu L, Xu X, Wang H, Ma X.** Glucagon-like peptide 1 potentiates glucotoxicity-diminished insulin secretion via stimulation of cAMP-PKA signaling in INS-1E cells and mouse islets. *Int J Biochem Cell Biol*. 2013;45(2):483–490.
15. **Ying Y, Li L, Cao W, et al.** The microtubule associated protein syntabulin is required for glucose-stimulated and cAMP-potentiated insulin secretion. *FEBS Lett*. 2012;586(20):3674–3680.
16. **Ronnebaum SM, Jensen MV, Hohmeier HE, et al.** Silencing of cytosolic or mitochondrial isoforms of malic enzyme has no effect on glucose-stimulated insulin secretion from rodent islets. *J Biol Chem*. 2008;283(43):28909–28917.
17. **Tomas A, Yermen B, Min L, Pessin JE, Halban PA.** Regulation of pancreatic β-cell insulin secretion by actin cytoskeleton remodelling: role of gelsolin and cooperation with the MAPK signalling pathway. *J Cell Sci*. 2006;119(Pt 10):2156–2167.
18. **Kalwat MA, Yoder SM, Wang Z, Thurmond DC.** A p21-activated kinase (PAK1) signaling cascade coordinately regulates F-actin remodeling and insulin granule exocytosis in pancreatic β cells. *Biochem Pharmacol*. 2013;85(6):808–816.
19. **Pellegrin S, Mellor H.** Actin stress fibres. *J Cell Sci*. 2007;120(Pt 20):3491–3499.
20. **Leung T, Chen XQ, Manser E, Lim L.** The p160 RhoA-binding kinase ROK α is a member of a kinase family and is involved in the reorganization of the cytoskeleton. *Mol Cell Biol*. 1996;16(10):5313–5327.
21. **Hammar E, Tomas A, Bosco D, Halban PA.** Role of the Rho-ROCK (Rho-associated kinase) signaling pathway in the regulation of pancreatic β-cell function. *Endocrinology*. 2009;150(5):2072–2079.
22. **Kawano Y, Fukata Y, Oshiro N, et al.** Phosphorylation of myosin-binding subunit (MBS) of myosin phosphatase by Rho-kinase in vivo. *J Cell Biol*. 1999;147(5):1023–1038.
23. **Shawl AI, Park KH, Kim BJ, Higashida C, Higashida H, Kim UH.** Involvement of actin filament in the generation of Ca2+ mobilizing messengers in glucose-induced Ca2+ signaling in pancreatic β-cells. *Islets*. 2012;4(2):145–151.
24. **Jewell JL, Luo W, OH E, Wang Z, Thurmond DC.** Filamentous actin regulates insulin exocytosis through direct interaction with Syntaxin 4. *J Biol Chem*. 2008;283(16):10716–10726.
25. **Qiao J, Huang F, Lum H.** PKA inhibits RhoA activation: a protection mechanism against endothelial barrier dysfunction. *Am J Physiol Lung Cell Mol Physiol*. 2003;284(6):L972–L980.
26. **Laudanna C, Campbell JJ, Butcher EC.** Elevation of intracellular cAMP inhibits RhoA activation and integrin-dependent leukocyte adhesion induced by chemoattractants. *J Biol Chem*. 1997;272(39):24141–24144.
27. **Zhou H, Li YJ.** Rho kinase inhibitors: potential treatments for diabetes and diabetic complications. *Curr Pharm Des*. 2012;18(20):2964–2973.
28. **Eliasson L, Ma X, Renstrom E, et al.** SUR1 regulates PKA-independent cAMP-induced granule priming in mouse pancreatic B-cells. *J Gen Physiol*. 2003;121(3):181–197.
29. **Seino S.** Cell signalling in insulin secretion: the molecular targets of ATP, cAMP and sulfonylurea. *Diabetologia*. 2012;55(8):2096–2108.
30. **Riento K, Guasch RM, Garg R, Jin B, Ridley AJ.** RhoE binds to ROCK I and inhibits downstream signaling. *Mol Cell Biol*. 2003;23(12):4219–4229.
31. **Lang P, Gesbert F, Delespine-Carmagnat M, Stancou R, Pouchelet M, Bertoglio J.** Protein kinase A phosphorylation of RhoA mediates the morphological and functional effects of cyclic AMP in cytotoxic lymphocytes. *EMBO J*. 1996;15(3):510–519.
32. **Amano M, Ito M, Kimura K, et al.** Phosphorylation and activation of myosin by Rho-associated kinase (Rho-kinase). *J Biol Chem*. 1996;271(34):20246–20249.
33. **Malmgren S, Spegel P, Danielsson AP, et al.** Coordinate changes in histone modifications, mRNA levels, and metabolite profiles in clonal INS-1 832/13 β-cells accompany functional adaptations to lipotoxicity. *J Biol Chem*. 2013;288(17):11973–11987.